G. Consolati, G. Panzarasa, F. Quasso
Morphology of Free Volume Holes in an Amorphous Polyether-Polyester Polyurethane of Biomedical Interest
Polymer Testing, Vol. 68, 2018, p. 208-212
doi:10.1016/j.polymertesting.2018.04.016

Contents lists available at ScienceDirect

Polymer Testing

journal homepage: www.elsevier.com

Material Behaviour

Morphology of free volume holes in an amorphous polyether-polyester polyurethane of biomedical interest

Giovanni Consolati[a, b, *], Guido Panzarasa[c, 1], Fiorenza Quasso[a]

[a] Department of Aerospace Science and Technology, Politecnico di Milano, Via LaMasa, 34, 20156, Milano, Italy
[b] INFN, Sezione di Milano, Via Celoria, 16, 20133, Milano, Italy
[c] Department of Polymer Engineering and Science, Montanuniversität, Otto-Glöckel Straße 2, 8700, Leoben, Austria

ARTICLE INFO

Keywords:
Dilatometry
Free volume
Polyurethanes
Positron annihilation

ABSTRACT

Positron annihilation lifetime spectroscopy (PALS) is a valuable technique for assessing the typical sizes of free volume holes in polymers. By coupling the results obtained from the positron annihilation spectra with those supplied by dilatometry, more precise information can be extracted on the free volume fraction and novel insight can be acquired on the shapes of the holes, demonstrating the limitations of the spherical approximation. In the present paper, we apply the combined PALS-dilatometry approach to study an amorphous polyether-polyester polyurethane, a polymer of great technological interest. We find that flattened and elongated holes, rather than spherical ones, better account for the behavior of the free volume fraction as a function of the temperature.

1. Introduction

The free volume concept [1,2] accounts for several features of polymers, such as diffusivity of permeants, mechanical and viscoelastic properties. Aging effects can as well be explained in terms of changes in the free volume [3]. Experimental assessment of the free volume is consequently of the utmost importance, for theoretical reasons as well as for practical purposes, especially to develop polymers with well-controlled properties. Among the few experimental techniques which enable to extract information on the microscopic structure of the free volume (such as small angle X-ray diffraction [4], the use of photochromic labels [5] and photoisomerization [6]), positron annihilation lifetime spectroscopy (PALS) [7] has become one of the most popular, thanks to its non-destructive character (as discussed in the Supplemental File) and because it does not require the use of permanent external probes, which could introduce some systematic bias [6]. In the case of PALS, the probe is positronium, Ps, an unstable bound state which may be formed when a positron introduced in the sample and rapidly thermalized encounters an electron of the analyzed medium. Ps has the same size of the hydrogen atom [8] but it is about two thousand times lighter. In fact, the Bohr radius of Ps is twice that of hydrogen, since the reduced mass of Ps is one half of that of the electron; however, both the electron and positron rotate around the common center of mass. The diameter of the two systems is therefore the same. Because it is repelled from the medium itself, due to the exchange repulsion between the Ps electron and the electrons belonging to the surroundings, positronium is an 'hole seeker'. It means that Ps localizes preferably in the open spaces of the host structure, such as the free volume holes in the amorphous zones and the defects present in the crystalline regions (in the case of semicrystalline polymers). Ground state Ps exists in two sublevels, according to different spin orientations: para-Ps (p-Ps, antiparallel spins) and ortho-Ps (*o*-Ps, parallel spins) [9]. Being the positron and the electron antiparticles of each other, they annihilate by transforming their mass into photons, according to the equivalence between mass and energy. This makes Ps an almost ideal probe for investigating free volume holes, if Ps lifetime is short with respect to that of dynamic holes.

The lifespan of Ps is spin-dependent: in a vacuum, p-Ps annihilates by emitting two photons with a lifetime of 125 ps, while the *o*-Ps lifetime is 142 ns and three annihilation photons are emitted. Inside a hole, *o*-Ps interacts with the surrounding electrons for a time interval

* Corresponding author. Department of Aerospace Science and Technology, Politecnico di Milano, Via LaMasa, 34, 20156, Milano, Italy.
Email addresses: giovanni.consolati@polimi.it (G. Consolati); gp4779@gmail.com (G. Panzarasa); fiorenza.quasso@polimi.it (F. Quasso)
[1] Present address: Laboratory for Soft and Living Materials, Department of Materials, ETH Zürich, Vladimir-Prelog-Weg 5, 8093, Zürich, Switzerland.

https://doi.org/10.1016/j.polymertesting.2018.04.016
Received 18 January 2018; Received in revised form 22 March 2018; Accepted 13 April 2018
Available online xxx
0142-9418/

long enough to make possible annihilation with an 'external' electron in a relative singlet spin state. This process, called 'pickoff annihilation', decreases the lifetime of *o*-Ps compared to its value in a vacuum. The magnitude of the decrease depends on the overlap between the wavefunctions of the positron and of the surrounding electrons. In other words, the smaller the size of the holes the lower the lifetime. This correlation between *o*-Ps lifetime and hole size is the essence of PALS applications to soft matter and, especially, to polymers. On the other hand, the lifetime of p-Ps is only slightly affected passing from vacuum to matter, since the pickoff decay rate (generally lower than 1 ns^{-1}) is at least one order of magnitude lower than the intrinsic decay rate (8 ns^{-1}). For this reason only the *o*-Ps component is generally considered for free volume investigations.

The knowledge of two quantities, the average volume of the holes v_h and their number density N, is necessary to estimate the specific free volume V_f, as expressed in equation (1) [10]:

$$V_f = N v_h \tag{1}$$

Therefore, it is necessary to convert the *o*-Ps lifetime into a hole size, which implies that a suitable geometry for the holes has to be assumed. This is mandatory to convert the raw results of PALS measurements into a quantitative information. The use of conventional geometries is a common feature to many experimental techniques: for instance, in the case of nitrogen porosimetry technique, cylindrical, or even slit-shaped pores, are often assumed [11]. The most used geometry for PALS studies in polymers is the spherical one [12,13], although alternative shapes were sometimes considered. Indeed, ellipsoidal cavities were introduced [14] to frame free volume holes in a semicrystalline polyether ether ketone (PEEK), subjected to tensile deformation and cylindrical voids were assumed among the chains in syndiotactic polystyrene [15]. Cuboids were also introduced [16] to better represent voids in some molecular crystals. It is also worth mentioning that computer simulations on the free volume were performed, since the pioneering work by Rigby and Roe [17]. With the increase of complexity of algorithms several features of the investigated materials from first principles were obtained, including the geometrical shape of the free volume holes. A complex picture then appears, depending on the specific structure. If in soft polymers the spherical shape seems the suitable one [18], in poly(ethylene)-like macromolecules non-spherical shapes become important on increasing the size of the free volume hole [19]. In stiff chain polymers cigar-like holes seem to be more common than spherical ones [20]. Non-spherical (elongated) shapes were found also in a molecular dynamics study of poly(vinyl methylether) [21].

For a given o-Ps lifetime, different geometries may produce significant differences in the calculated volumes of the holes and thus of free volume [22]. If this last parameter has to be precisely evaluated, it is necessary to discriminate, among the different possible morphologies of the holes, the one that is the most suitable for the polymer under study.

In the present work, we show how this can be obtained by coupling the results supplied by PALS and dilatometry and comparing the free volume fraction as given by the experiment with that supplied by the lattice-hole theory [23]. We studied an amorphous polyester-polyether polyurethane, poly[4,4′-methylenebis(phenyl isocyanate)-*alt*-1,4-butanediol/di(propylene glycol)/polycaprolactone] (PMI). This class of polymers is of great technological interest, as it combines the properties of both polyester- and polyether-polyurethanes, such as good flexibility at low temperatures, excellent hydrolytic stability, high tensile strength and good heat resistance. Moreover, PMI shows good bio- and blood-compatibility, making it particularly suitable for clinical applications [24]. To the best of our knowledge, this is the first time that PMI is investigated by means of PALS.

2. Experimental

Poly[4,4′-methylenebis(phenyl isocyanate)-*alt*-1,4-butanediol/di(propylene glycol)/polycaprolactone] is a methylene-diisocyanate (MDI)-polyester-polyether polyurethane whose chemical structure is represented in Fig. 1. It was purchased from Sigma-Aldrich (CAS number: 68084-39-9) in the form of pellets, which were converted in slabs by compression molding.

Thermal analysis was carried out by means of a Mettler-Toledo DSC 822e differential scanning calorimeter, calibrated with high purity indium standard. Samples (about 5 mg) were encapsulated in aluminum pans and heated from 193 to 273 K at a rate of 2 K min^{-1} under nitrogen flux.

Specific volume of PMI was initially determined at 300 K as the inverse of the density ρ, measured by means of a Sartorius balance (model ME215P: readability 10^{-5} g, repeatability $1.5 \cdot 10^{-5}$ g), equipped with a kit for the measurement of the density. It resulted to be $\rho = 1.1620\ g\ cm^{-3}$.

Accurate specific volume measurements were carried out by means of a capillary dilatometer (bulb volume: 2.306 cm^3, capillary length: 30 cm, capillary section: 0.0143 cm^2), containing the sample surrounded by mercury (purity > 99.999%, Fluka) used as a reference liquid. The temperature cooling runs were carried out by immerging the filled dilatometer in a thermostatic bath; water in the temperature range 315–280 K and ethanol (temperature range 280–249 K) were used as circulating liquids. The minimum temperature reachable by the bath was 249 K. The mercury meniscus height into the capillary was determined by means of a cathetometer with digital reading. Minimal stability of the temperature was within 0.5 K. Three runs were carried out; the determination of the specific volume at any temperature resulted from an average of the corresponding values found in each measurement. Each temperature was reached by cooling the sample from the previous temperature at a rate of 0.1 K min^{-1} up to the new tem-

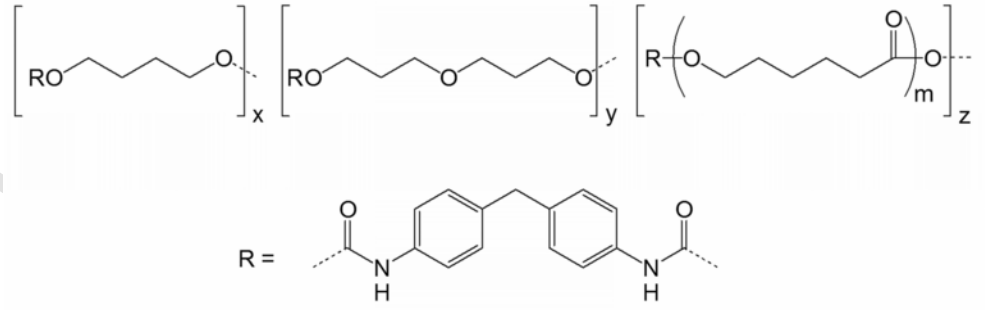

Fig. 1. Chemical structure of the investigated polyether-polyester polyurethane.

perature. Then, the sample was allowed to remain in the new temperature state for 1000 s before starting the measurements. The same procedure was followed for PALS measurements. This granted that the obtained values of specific volumes and free volumes above the glass transition, as obtained in PMI, were not affected by the experimental protocol, since typical relaxation times for polymers around T_g is of the order of 100 s [25] and decrease by orders of magnitude by increasing the temperature.

PALS measurements were carried out on square samples (surface area: 4 cm^2). Their thickness (2 mm) was sufficient to stop all the injected positrons. Smaller pieces cut from the same batch were used for the measurement of the specific volume. The positron source, ^{22}Na enveloped between two identical Kapton® foils (thickness 7.6 μm each) was placed in the center of a small copper cup containing the sample and in direct contact with the heat exchanger of a liquid nitrogen cryostat (DN 1714 Oxford Instruments). Stability of the temperature was ensured within 0.5 K. All the measurements were carried out in a vacuum: before starting the measurements the sample was evacuated for 12 h. Positron annihilation lifetime spectra were collected through a conventional fast–fast coincidence setup having a resolution of about 280 ps. Each spectrum, containing about $2{\cdot}10^6$ counts, was acquired in a few hours and analyzed through the computer code *LT* [26], with a suitable correction for the positrons annihilated in Kapton. Three spectra for each temperature were collected.

3. Results and discussion

Dilatometric data are shown in Fig. 2. A linear trend of the specific volume V is observed in the range of investigated temperatures; the straight line is the result of a fit with a correlation coefficient >0.999. From the dilatometric data we can estimate the free volume fraction h in PMI, within the framework of the Simha-Somcynsky theory [23]. The equation of state given by this approach is valid for amorphous polymers at equilibrium [27]; at atmospheric pressure it assumes the form of the two following coupled equations:

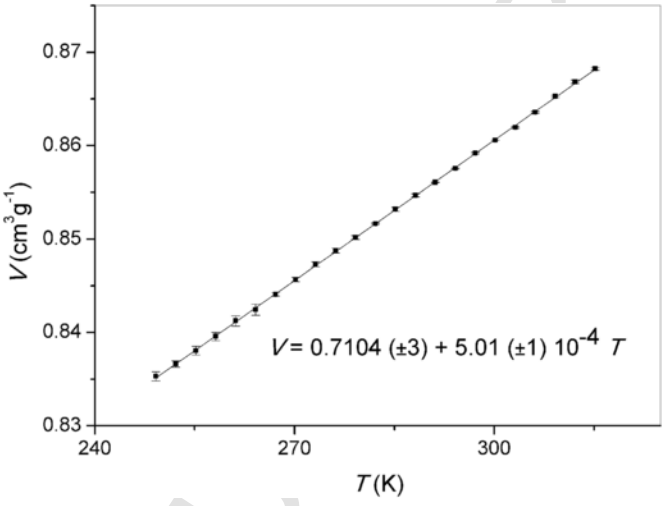

Fig. 2. Specific volume V as a function of the temperature T in PMI. For certain data points experimental uncertainties are within the symbols.

$$\widetilde{T} = 2y\left(y\widetilde{V}\right)^{-2}\left[1.2045 - 1.011\left(y\widetilde{V}\right)^{-2}\right]\left[1 - 2^{-1/6}y\left(y\widetilde{V}\right)^{-1/3}\right]; \tag{2a}$$

$$1 + y^{-1}\ln(1-y) = \left(y/6\widetilde{T}\right)\left(y\widetilde{V}\right)^{-2}\left[2.409 - 3.033\left(y\widetilde{V}\right)^{-2}\right] + \left[2^{-1/6}y\left(y\widetilde{V}\right)^{-1/3} - (1/3)\right]\left[1 - 2^{-1/6}y\left(y\widetilde{V}\right)^{-1/3}\right]^{-1} \tag{2b}$$

which are expressed in terms of the reduced thermodynamic coordinates

$$\widetilde{T} = T/T^*$$

and

$$\widetilde{V} = V/V^*$$

where T^* and V^* are scaling parameters which depend on the material. The parameters T^* and V^* result from a simultaneous fitting procedure of equations (2a) and (2b) to the data shown in Fig. 1; otherwise, a simpler interpolation expression can be used [28]. The two procedures produce almost identical results at atmospheric pressure [29]. Concerning PMI, it results $V^* = 0.8453 \pm 1\,cm^3g^{-1}$ and $T^* = 10144 \pm 32\,K$. The hole fraction h is derived from equations (2a) and (2b); it can be interpreted as a free volume fraction which relates to typical transport properties, such as the constant stress viscosity of melts and their mixtures [30]. Furthermore, its connection with PALS results has been demonstrated [31]. In the range of temperatures investigated in the present work ($0.0245 < T/T^* < 0.0311$) the behavior of the hole fraction versus temperature is linear (see Fig. 5).

Positron annihilation lifetime spectra were successfully analyzed in three components; the χ^2 test supplied values in the range 0.93–1.11. The shortest lifetime component is attributed to positrons annihilating in the bulk as well as to para-Ps annihilations. This last contribution cannot be resolved as a distinct component, owing to both the resolution of the apparatus and the intensity of the signal itself, which can be expected to be of the order of one third of the longest lifetime component. The intermediate component originates from positrons annihilating into defects and free volume holes; their lifetime is higher than the shortest one since the electron density surrounding the positron is lower with respect to the bulk. The longest component is attributed to the decay of *o*-Ps trapped in the free volume holes. Fig. 3 shows the *o*-Ps lifetime τ_3 as a function of temperature.

In the temperature region below 230 K there is a moderate increase of the lifetime τ_3, while above 240 K there is a sharp increase with T. The change of the slope of *o*-Ps lifetime versus the temperature, $\frac{d\tau_3}{dT}$, corresponds to the glass transition; the associated temperature T_g can be conventionally obtained as the intersection point of the two straight lines fitting the data. It results $T_g = 229\,K$, in good agreement with the value supplied by differential scanning calorimetry (233 K). Therefore, the behavior of τ_3 mirrors that of the free volume: below T_g the inter-

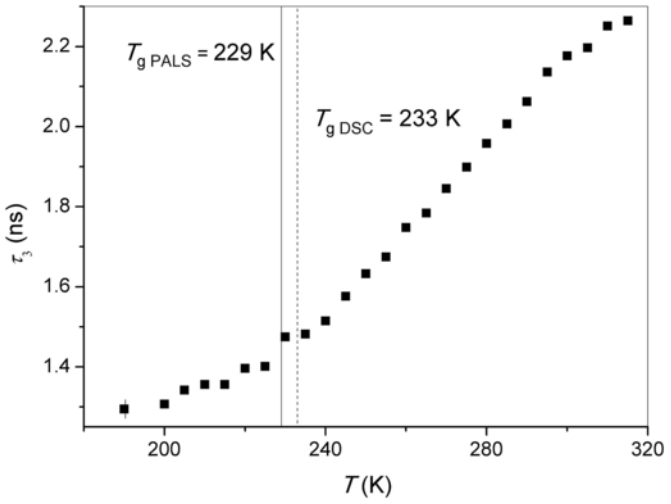

Fig. 3. Evolution of the *o*-Ps lifetime in PMI as a function of the temperature. The vertical lines correspond to the glass transitions as measured by PALS and DSC. Typical uncertainty is reported in the first data point.

chain motions are strongly hindered and the expansion coefficient of the free volume is smaller than above T_g where the chain segments become mobile: the free volume increases with temperature at a higher rate. The slightly lower value of T_g as obtained from PALS with respect to DSC can be attributed to the different cooling rates used in the two techniques.

Above 300 K a reduced increase of τ_3 with temperature is visible. This trend is commonly observed in many polymers and various explanations were proposed: (i) formation of a Ps bubble [32], (ii) digging of holes by Ps itself [33] or (iii) a relaxation time of the molecular chains which is comparable to Ps lifetime [34]. In this last case Ps would not be any longer able to correctly probe the size of the host cavity. Whatever the adopted explanation, there is a general agreement on the contention that in this temperature region Ps cannot give reliable information on the free volume hole [35]. Therefore, we will limit our discussion to temperatures below 300 K.

Lifetime values as those shown in Fig. 3 are generally converted into average sizes of the free volume holes by using the Tao-Eldrup equation (3) [12,13], with the assumption that the cavity hosting Ps is a spherical void with effective radius R. Such a Ps trap has a potential well with finite depth. However, for convenience of calculations the depth is considered to be infinite but the radius is increased to $R + \Delta R$, where ΔR (= 0.166 nm) is an empirical parameter [13,36] which describes the penetration of the Ps wave function into the bulk. The electron density is supposed to be zero for $r < R$ and constant for $r > R$. The relationship between the *o*-Ps pickoff decay rate λ_p and R is the following:

$$\lambda_p = \lambda_0 \left[\frac{\Delta R}{R + \Delta R} + \frac{1}{2\pi} \sin\left(2\pi \frac{R}{R + \Delta R}\right) \right] \tag{3}$$

where λ_0 ? 2 ns^{-1} is the annihilation rate of *o*-Ps in the presence of a high electron density, which results from the spin-averaged annihilation rate of *p*-Ps and *o*-Ps in a vacuum.

The *o*-Ps lifetime τ_3 is the reciprocal of the total decay rate λ_3, which is the sum of the pickoff decay rate and the intrinsic decay rate $\lambda_i = 1/142$ ns^{-1}:

$$\tau_3 = 1/\lambda_3 = 1/\left(\lambda_p + \lambda_i\right) \tag{4}$$

The last term generally represents a negligible correction: in a good approximation *o*-Ps lifetime in a free volume hole of common polymers can be assumed to be the inverse of the pickoff decay rate.

Other relationships can be deduced between τ_3 and the typical size of a cavity having a different shape with respect to the spherical one [14,15,37]. Using the spherical geometry we calculate the hole volume as $v_h = \frac{4}{3}\pi R^3$, where R is obtained from equation (3).

Specific volume is then given by Ref. [38]:

$$V = N v_h + V_{occ} \tag{5}$$

where V_{occ} is the occupied specific volume, i.e. the sum of the Van der Waals volume and the interstitial free volume [39]:

$$V_{occ} = V_{vdw} + V_{if}$$

In fact, interstitial free volume consists of local empty spaces which are too small to localize even a small probe such as Ps and it is associated to the occupied volume. The S-S theory predicts a dependence of the occupied volume on the temperature which reflects the expansion of the interstitial free volume [28]; however, the thermal expansion coefficient is of the order of 3×10^{-5}K^{-1}. Therefore, in the range of temperatures investigated in the present study we assumed the specific occupied volume V_{occ} to be constant.

The free volume V_f is an 'excess' free volume accessible to Ps and it is the one calculated as the hole fraction h in the lattice-hole theory [39].

Fractional free volume f is evaluated according to the definition:

$$f = \frac{V_f}{V} = \frac{N v_h}{N v_h + V_{occ}}. \tag{6}$$

By coupling PALS and dilatometric data we can find both N and V_{occ} through the fitting procedure shown in Fig. 4, where V is plotted versus v_h in a suitable range of temperatures.

Fig. 4 shows that the specific volume V is a linear function of the average hole volume v_h, calculated with the spherical approximation: the data are fitted by a straight line (also shown in Fig. 4) and the correlation coefficient is 0.996. According to eq. (5), a linear relationship implies constancy of parameters N (slope) and V_{occ} (intercept at the origin). The physical consequence is that N can be assumed constant for

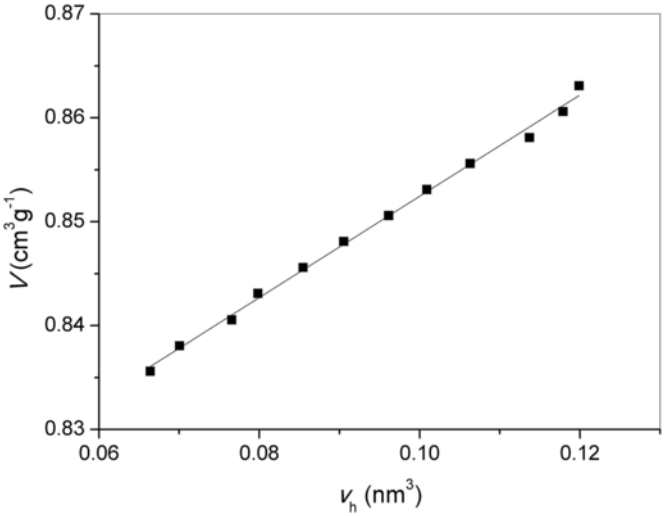

Fig. 4. Specific volume V versus the hole volume v_h in PMI.

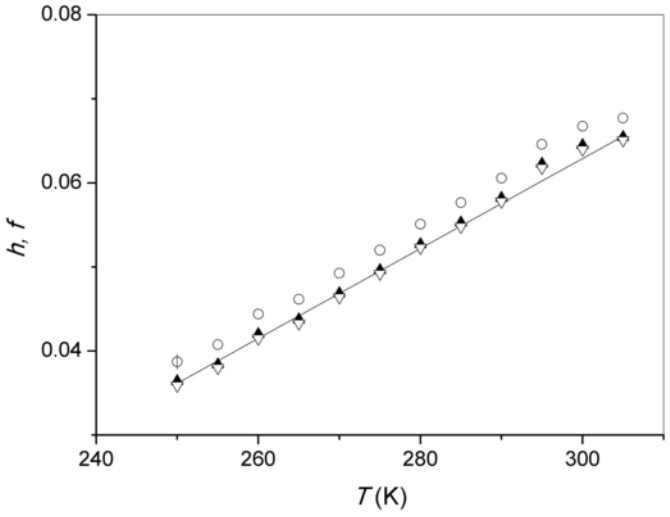

Fig. 5. Free volume fraction f as obtained from PALS and dilatometric data, by considering holes as spheres (empty circles), flattened cuboids (full triangles) or elongated cuboids (empty triangles). Flattened (aspect ratio 0.48) or elongated (aspect ratio 3.4) cuboids produce the same free volume fraction. The continuous line represents the free volume fraction h, as calculated from the lattice-hole model. Typical uncertainty is reported in the first data point.

the analyzed PMI, at least above the glass transition and in the range of investigated temperatures. It results $N = 4.9\ 10^{20}\,g^{-1}$.

A linear correlation is produced also by assuming a non-spherical geometry, too, although with different values for N and V_{occ}. The specific volume was evaluated at the same temperature of positron data by using a linear interpolation from the data shown in Fig. 2.

Once obtained N and V_{occ} the free volume fraction f (equation (6)) was calculated for a given hole geometry. Its behavior versus the temperature is shown in Fig. 5 together with the theoretical free volume fraction h. Values of f obtained using a spherical cavity geometry (empty circles in Fig. 4) are systematically higher than h; furthermore, expansion coefficients of f are slightly higher than the corresponding theoretical values.

The discrepancy between f and h can be solved by choosing a different morphology for the free volume holes. By approximating the holes as cuboids, for simplicity with square section, and introducing the ratio k between the height and the size of the base of the cuboid, we found that flattened cuboids ($k = 0.48$, full circles in Fig. 5) produce a very satisfactory agreement between the theoretical and the 'experimental' determinations of the free volume fraction. Also elongated cuboids ($k > 1$) produce agreement between f and h; but in this case the best fit is obtained with a rather high aspect ratio, $k = 3.4$. The flattened/elongated morphology does not seem to depend on the geometry chosen; in fact, almost the same results are found by treating the holes as finite cylinders [15] with aspect ratio $q = 0.43$ (flattened) or $q = 3$ (elongated), which are very similar (within 10%) to the values found for k. It is worth to note that molecular dynamics simulations performed in poly(vinyl methylether) [40] suggest that aspect ratios of elongated holes do not change with temperature, in agreement with our present finding.

A χ^2 test (where normalized $\chi^2 = \frac{1}{d}\sum_{i=1}^{n}\left(\frac{f(i)-h(i)}{\sigma_i}\right)^2$, d = number of degrees of freedom, σ_i = uncertainty associated to the i-th measurement, n = number of measurement) [41] gave in the case of spherical holes $\chi^2 = 5.3$, while for flattened cuboids $\chi^2 = 0.41$ and for elongated ones $\chi^2 = 0.36$.

The free volume fraction extrapolated at the glass transition, calculated using the spherical geometry for holes supplies a value (2.67%) which is higher than the one estimated on the basis of the lattice-hole theory (2.49%). On the other hand, almost the same value (2.46%) is obtained using flattened or elongated geometries for the holes.

4. Conclusions

Amorphous polyester-polyether polyurethanes are widely used for their favorable technological properties. However, a detailed characterization in terms of free volume is lacking. In the present work, we contributed to fill this knowledge gap by studying poly[4,4′-methylenebis(phenyl isocyanate)-*alt*-1,4-butanediol/di(propylene glycol)/polycaprolactone] (PMI). The results of dilatometry and PALS were used to deduce a more precise value of the free volume fraction at the glass transition temperature as well as to get insight on the morphology of the free volume holes present in the polymer. In fact, despite the irregular shape of real holes, we found that flattened or elongated cavities, with aspect ratio of the order of 0.5 and 3, respectively, are more suitable models for free volume holes in PMI compared to spheres. More than the specific geometry (cuboids or cylinders), our findings address towards a morphology which allows a better representation of the free volume fraction. Presently, we cannot discriminate between a flattened or elongated morphology. Valuable help could come from computer simulations; as already mentioned, insights on shapes of the holes can be obtained by suitable algorithms. They seem to suggest elongated holes as preferred geometries, but detailed investigations are needed for each kind of polymer. Different factors could contribute to non spherical morphology, including preparation of the sample (by compression molding, in our case). We also point out the importance of dilatometry to increase the accuracy of such measurements, both because it supplies the thermodynamic parameters needed to evaluate the theoretical free volume fraction, and because it is only through a combination of PALS and dilatometry that it is possible to compare various possible geometries of the holes and choose the most suitable ones.

Although obtained for a specific polymer, the described methodology has a general value since it can be applied to any amorphous polymer at equilibrium.

Acknowledgments

G.C. is grateful to Prof. J. Bartoš (Slovak Academy of Sciences) for useful discussions.

References

[1] Y.C. Jean, in: A. Dupasquier, A.P. Mills (Eds.), Positron Spectroscopy of Solids, OIP Press, Amsterdam, 1995, pp. 563–580.
[2] D. Turnbull, M.H. Cohen, J. Chem. Phys. 34 (1961) 120.
[3] G.M. Odegard, A. Bandyopadhyay, J. Polym. B, Part B: Polym. Phys. 49 (2011) 1695.
[4] R.J. Roe, H.H. Song, Macromolecules 18 (1985) 1603.
[5] L. Lamarre, C.S.P. Sung, Macromolecules 16 (1983) 1729.
[6] J.G. Victor, J.M. Torkelson, Macromolecules 20 (1987) 2241.
[7] Y.C. Jean, J.D. Van Horn, W.-S. Hung, K.-R. Lee, Macromolecules 46 (2013) 7133.
[8] Y.C. Jean, P.E. Mallon, D.M. Schrader, in: Y.C. Jean, P.E. Mallon, D.M. Schrader (Eds.), Principles and Applications of Positron and Positronium Chemistry, World Scientific, New Jersey, 2003, p. 4.
[9] D.M. Schrader, Y.C. Jean, in: D.M. Schrader, Y.C. Jean (Eds.), Positron and Positronium Chemistry, Elsevier, Amsterdam, 1988, Ch. 1.
[10] G. Dlubek, J. Stejny, M.A. Alam, Macromolecules 31 (1998) 4574.
[11] S.J. Gregg, K.S.W. Sing, Adsorption, Surface Area and Porosity, Academic press, London, 1982.
[12] S.J. Tao, J. Chem. Phys. 56 (1972) 5499.
[13] M. Eldrup, D. Lightbody, N.J. Sherwood, Chem. Phys. 63 (1981) 51.
[14] Y.C. Jean, H. Shi, J. Non-Crys. Solids 172 (1994) 806.
[15] B.G. Olson, T. Prodpran, A.M. Jamieson, S. Nazarenko, Polymer 43 (2002) 6775.
[16] B. Jasińska, A.E. Kozioł, T. Goworek, J. Radioanal. Nucl. Chem. 210 (1996) 617.
[17] D. Rigby, R.J. Roe, Macromolecules 23 (1990) 5312.
[18] M. Sega, P. Jedlovsky, N.N. Medvedev, Vallauri, J. Chem. Phys. 121 (2004) 2422.
[19] H. Don, K.I. Jacob, Macromolecules 36 (2003) 8881.
[20] D. Hofmann, M. Entrialgo-Castano, A. Lerbret, M. Heuchel, Y. Yampolskii, Macromolecules 36 (2003) 8528.

[21] D. Račko, S. Capponi, F. Alvarez, J. Colmenero, J. Bartoš, J. Chem. Phys. 131 (2009), 064903.
[22] G. Consolati, J. Chem. Phys. 117 (2002) 7279.
[23] R. Simha, T. Somcynsky, Macromolecules 2 (1969) 342.
[24] Z. Hu, Z. Li, L. Hu, W. He, R. Liu, Y. Qin, S. Wang, BMC Cardiovasc. Disord. 12 (2012) 115.
[25] J. Bartoš, M. Iskrová - Miklošovicová, O. Šauša, D. Cangialosi, A. Alegría, H. Švajdlenková, J. Krištiak, A. Arbe, J. Colmenero, J.Phys. Cond. Matter 24 (2012), 155104.
[26] J. Kansy, Nucl. Instrum. Methods Phys. Res., Sect. A 374 (1996) 235.
[27] L.A. Utracki, Polymer 46 (2005) 11548.
[28] R. Simha, P.S. Wilson, Macromolecules 6 (1973) 908.
[29] L.A. Utracki, R. Simha Macromol, Chem. Phys. Mol. Theory Simul. 10 (2001) 17.
[30] L.A. Utracki, J. Rheol. 30 (1986) 829.
[31] Z. Yu, U. Yahsi, J.D. McGerwey, A.M. Jamieson, R. Simha, J. Polym. Sci., Part B: Polym. Phys. 32 (1994) 2637.
[32] P. Winberg, M. Eldrup, F.H.J. Maurer, J. Chem. Phys. 136 (2012), 244902.
[33] Y. Ito, H.F.M. Mohamed, K. Tanaka, K. Okamoto, K. Lee, J. Radioanal. Nucl. Chem. 211 (1996) 211.
[34] J. Bartoš, O. Šauša, J. Krištiak, T. Blochowicz, E. Rössler, J. Phys. Condens. Matter 13 (2001) 11473.
[35] J. Bartoš, A. Alegría, O. Šauša, M. Tyagi, D. Gómez, J. Krištiak, J. Colmenero, Phys. Rev. E 76 (2007), 031503.
[36] H. Nakanishi, S.J. Wang, Y.C. Jean, in: S.C. Sharma (Ed.), Positron Annihilation Studies of Fluids, World Scientific, Singapore, 1988, p. 292.
[37] B. Jasińska, A.E. Kozioł, T. Goworek, Acta Phys. Pol. 95 (1999) 557.
[38] R. Srithawatpong, Z.L. Peng, B.G. Olson, A.M. Jamieson, R. Simha, J.D. McGervey, T.R. Maier, A.E. Halasa, H. Ishida, J. Polym. Sci., Part B: Polym. Phys. 37 (1999) 2754.
[39] G. Dlubek, in: L.A. Utracki, A.M. Jamieson (Eds.), Polymer Physics. From Suspensions to Nanocomposites and Beyond, John Wiley & Sons, Singapore, 2010, pp. 421–472.
[40] D. Račko, S. Capponi, F. Alvarez, J. Colmenero, J. Chem. Phys. 134 (2011), 044512.
[41] J.R. Taylor, An Introduction to Error Analysis, second ed., University Science books, Sausalito, CA, 1997268.